



HAL
open science

eCOALIA: Neocortical Neural Mass Model for simulating electroencephalographic signals

E Köksal-Ersöz, M Yochum, P Benquet, F Wendling

► **To cite this version:**

E Köksal-Ersöz, M Yochum, P Benquet, F Wendling. eCOALIA: Neocortical Neural Mass Model for simulating electroencephalographic signals. 2024. hal-04711984

HAL Id: hal-04711984

<https://hal.science/hal-04711984v1>

Preprint submitted on 27 Sep 2024

HAL is a multi-disciplinary open access archive for the deposit and dissemination of scientific research documents, whether they are published or not. The documents may come from teaching and research institutions in France or abroad, or from public or private research centers.

L'archive ouverte pluridisciplinaire **HAL**, est destinée au dépôt et à la diffusion de documents scientifiques de niveau recherche, publiés ou non, émanant des établissements d'enseignement et de recherche français ou étrangers, des laboratoires publics ou privés.

1 eCOALIA: Neocortical Neural Mass Model for
2 simulating electroencephalographic signals

3 E. Köksal-Ersöz^{a,1,2}, M. Yochum^{a,1}, P. Benquet^a, F. Wendling^a

4 ^a*Univ Rennes, Inserm, LTSI U1099, Rennes, France.*

5 **Abstract**

6 This paper introduces eCOALIA, a Python-based environment for simulat-
7 ing intracranial local field potentials and scalp electroencephalography (EEG)
8 signals with neural mass models. The source activity is modeled by a novel
9 neural mass model respecting the layered structure of the neocortex. The
10 whole-brain model is composed of coupled neural masses, each representing a
11 brain region at the mesoscale and connected through the human connectome
12 matrix. The forward solution on the electrode contacts is computed using
13 biophysical modeling. eCOALIA allows parameter evolution during a simu-
14 lation time course and visualizes the local field potential at the level of cor-
15 tex and EEG electrodes. Advantaged with the neurophysiological modeling,
16 eCOALIA advances the *in silico* modeling of physiological and pathological
17 brain activity.

18 *Keywords:* neural mass modeling, whole-brain modeling, forward solution,
19 EEG, Python

20 **Metadata**

21 **1. Motivation and significance**

22 Electroencephalography (EEG) recordings are invaluable tools in clinical and
23 research settings, offering insights into the complexities of brain function.
24 From clinical diagnosis of neurological conditions to monitoring brain activ-
25 ity during surgeries, EEG plays a crucial role in healthcare. Beyond medical
26 applications, EEG is utilized in cognitive research to study attention, mem-
27 ory, and language while also serving as a cornerstone in the development
28 of brain-computer interfaces and neurofeedback therapy. With its ability to

¹co-first author

²corresponding author: elif.koksal-ersoz@inserm.fr

Nr.	Code metadata description	Please fill in this column
C1	Current code version	V1
C2	Permanent link to code/repository used for this code version	https://github.com/yymm2/eCOALIA
C3	Permanent link to Reproducible Capsule	
C4	Legal Code License	GNU GENERAL PUBLIC LICENSE Version 3, 29 June 2007
C5	Code versioning system used	git
C6	Software code languages, tools, and services used	python3.10 or 3.11
C7	Compilation requirements, operating environments & dependencies	PyQt6>=6.6.1, Numpy>=1.23.5, Scipy>=1.10.1, matplotlib>=3.8.3, vtk>=9.2.6
C8	Link to developer documentation/manual	https://github.com/yymm2/eCOALIA/blob/main/README.md
C9	Support email for questions	maxime.yochum@univ-rennes.fr

Table 1: Code metadata

29 map brain function and detect abnormalities, EEG stands at the forefront
30 of understanding the human brain and advancing medical treatments. How-
31 ever, deciphering the neurophysiological factors leading to electroencephalo-
32 graphic observations remains limited in humans due to the unavailability of
33 simultaneous multiscale (from single cells to populations of cells) recordings.
34 Computational modeling can fill this gap.
35 Whole-brain modeling has now become a standard method for *in silico* ex-
36 ploration of the healthy and pathological brain dynamics [1], and interpreta-
37 tion of the electrophysiological recordings. Whole-brain modeling tools have
38 made predictions between the electrophysiological recordings and simulations
39 based on the relation between excitation/inhibition [2], noise level, variations
40 on whole-brain connectivity matrices [3], or give insights on functional ac-
41 tivity and controllability [4, 5, 6, 7]. However, they are limited in detailing
42 neurophysiological factors leading to a typical type of transient activity.
43 The most common whole-brain modeling and multimodel imaging platform
44 is The Virtual Brain (TVB) [8, 9]. More recently, a Python package was
45 released for whole-brain modeling for simulating BOLD (blood-oxygen-level-
46 dependent) signals [10]. These tools face two main issues. First, they assume
47 that measured signals are either a direct reflection of the firing rate or mem-
48 brane perturbations, while the layered structure of the neocortex imposes
49 a more complex picture for the generation of electrophysiological signals.

50 Second, they focus on simulating oscillatory activity without accounting for
51 the physiology of transient signals, such as interictal epileptic discharges or
52 event-related potentials. eCOALIA addresses these issues with a neurophysi-
53 ologically plausible approach.

54 The groundbreaking nature of eCOALIA comes from the fact that it fol-
55 lows the layered structure of the neocortex and includes different inhibitory
56 and excitatory neuronal populations. In addition to simulating cortical os-
57 cillations, the model simulates signal morphology of transient events (in-
58 terictal epileptic discharges and event-related potentials) observed at the
59 level of EEG electrodes [11]. The implementation of the neocortical layered
60 structure allows distinguishing the layer-wise impact of the intra- and inter-
61 regional (cortico-cortical and subcortico-cortical) interactions on the signal
62 morphology. Therefore, eCOALIA can help to uncover the population-level
63 physiological mechanism leading to observed events. This generic model can
64 be developed further for patient-specific modeling and source localization of
65 EEG signals [12], for generating a large amount of data for training artificial
66 intelligence algorithms, and for optimization of brain stimulation technolo-
67 gies.

68 **2. Software description**

69 *2.1. Model description*

70 eCOALIA is based on a generic model of a neocortical region [11, 12], which
71 accounts for excitatory and inhibitory neuronal subpopulations found in the
72 neocortex. Each brain region is represented by the NMM given in (1) which
73 is connected to other brain regions according to the structural network of the
74 human brain; which combines axonal connections and propagation delays be-
75 tween regions. These connectivity matrices were generated using the Human
76 Connectome Project database [13] with Diffusion Tensor Imaging and Trac-
77 tography techniques. In particular, the connectivity matrices were created
78 using data from 487 adult subjects. Fractional anisotropy values were ex-
79 tracted from each subject and then averaged. These connectivity matrices
80 represent the strength of the connections between neural masses. The delay
81 matrix, which represents the time it takes for signals to travel between re-
82 gions, was calculated using a distance matrix multiplied by an average signal
83 propagation velocity of 7.5 m/s [14].

84 The generic NMM accounts for the firing rate, synaptic kinetics and con-
85 nectivity between the subpopulations. The post-synaptic potential (PSP)
86 emitted by a single neuronal subpopulation i in a particular brain region K

87 reads:

$$\ddot{y}_{K,i} = \frac{W_{K,i}}{\tau_{w_{K,i}}} \left(S \left(\sum_{K,j} C_{\{K,j\} \rightarrow \{K,i\}} y_{K,j} + \sum_{M,j} C_{\{M,j\} \rightarrow \{K,i\}} y_{M,j} \right) \right) \quad (1)$$

$$- \frac{2}{\tau_{w_{K,i}}} \dot{y}_{K,i} - \frac{1}{\tau_{w_{K,i}}^2} y_{K,i} + \frac{W_{K,i}}{\tau_{w_{K,i}}},$$

88 where $W_{K,i}, \tau_{w_{K,i}}$ are PSP amplitude and time constant, $C_{\{K,j\} \rightarrow \{K,i\}}$ is the
 89 coupling coefficient calibrating the afferent PSP from a subpopulation $\{K, j\}$
 90 within the region K and $C_{\{M,j\} \rightarrow \{K,i\}}$ from a subpopulation $\{M, j\}$ within the
 91 region M . The sigmoidal transfer function $S(\cdot)$ relates the membrane pertur-
 92 bations of the subpopulation $\{K, i\}$ due to incoming signals to its firing rate.
 93 The NMM representing a neocortical column integrates two excitatory subpop-
 94 ulations (P (P) and P' ($P1$)), and four types of inhibitory interneurons (i.e.,
 95 neuroglia form cells (NGFC), vasoactive intestinal peptide (VIP), parvalbu-
 96 min (PV) and somatostatin (SST) positive interneurons), represented by six
 97 subpopulations (PV ($I1$), PV' ($I1b$), SST ($I2$), VIP ($I3$), NGFC ($I4$) and
 98 NGFC' ($I4$)). The NMM representing the thalamus integrates one excita-
 99 tory subpopulations (thalamic nucleus cells (TC)) and two types (slow and
 100 fast) of inhibitory neuronal subpopulations (reticular neurons ($RT1, RT2$)).
 101 All the subpopulations within the region K can receive inputs from the exci-
 102 tatory subpopulation of the region M (subpopulation P for the neocortical
 103 regions and subpopulation TC for the thalamus). The model is schematized
 104 in Figure 1 and the model equations are given in Supplementary Material.
 105 The model equations are integrated using the Euler–Maruyama integration
 106 scheme [15] which is suitable when model incorporates statistical phenomenon.

107 2.2. Forward problem

108 The source activity (model output) is computed from the synaptic inputs
 109 targeting the layer V excitatory neurons. The macroscale EEG signal is
 110 computed using the current dipole approximation [16, 17]:

$$\phi(r) = \frac{1}{4\sigma\pi} \frac{\sum_{n=1}^M I_n^{axial}(t) \vec{d}_n \cos(\theta)}{|r - r_{source}|^2}, \quad (2)$$

111 where $I_n^{axial}(t) = \eta y(t)$ is an axial current along the vector \vec{d}_n at r_{source} and
 112 $\cos(\theta)$ is the angle between \vec{d}_n and the distance vector from the source
 113 and the electrode E. The parameter σ is the conductivity of the extracellular
 114 milieu and $\eta = 10^{-3} S$ is a conversion factor relating the PSP to postsynaptic
 115 current [18].

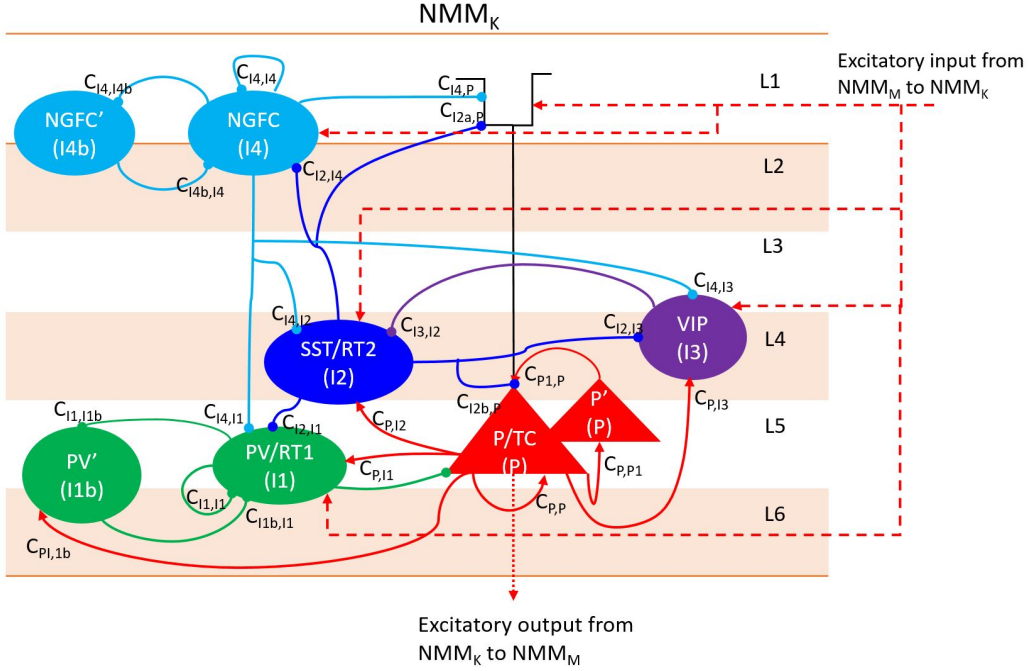


Figure 1: Single NMM with the labels of the subpopulations and connectivity coefficients as coded in eCOALIA.

116 The simulated source activity defines a time series, S of $N_R \times T$ matrix,
 117 N_R being the number of brain regions and T the size of the time vector
 118 of the simulated activity. eCOALIA uses the Colin head model [19] and
 119 Desikan Atlas [20] with $N_R = 66$ neocortical regions, which are available on
 120 Brainstorm [21]. A lead field matrix A ($66 \times N_E$), generated from 3-layer
 121 Boundary Element Method (BEM) model [22, 23], was used to compute the
 122 projection of the source activity onto the N_E number of EEG contacts. The
 123 X ($N_E \times T$) matrix of simulated EEG signals is obtained by $X = AS$.

124 2.3. Software architecture

125 The software was designed to be used via a Python script that instanti-
 126 ate a Cortex model which represents the brain with its interacting regions
 127 each modeled by a NMM. The user can load a simulation file or can modify
 128 the cortex model directly. It is possible to integrate parameter variations
 129 along the simulation as well as stimulation signals that account for electrical
 130 stimulation therapies (deep brain stimulation or transcranial electrical stim-
 131 ulation). Some visualization tool can be used to display the source LFP and
 132 EEG time series and their spectrograms. A 3D view allows also to display
 133 the LFP onto a 3D mesh of the cortex. Parameter evolution and stimulation

134 can be displayed as well. The use of scripts gives the flexibility for employing
135 user-specific routines and fine tuning of the simulation.

136 The provided documentation for the software package offers comprehensive
137 explanations and illustrative examples for using classes and functions. This
138 includes instantiating of a model, tuning parameters, conducting simulations,
139 and visualizing results.

140 The software package includes two scripts for performing single node ($N_{NMM} =$
141 1) and whole brain ($N_{NMM} = 67 - 1$ thalamic and 66 neocortical regions)
142 simulations, and one script for creating a network from scratch:

143 • Single node simulation: a Python script is available on the repository
144 to simulate a single node simulation starting from a previously saved
145 simulation file. The node's parameters can be changed and an external
146 stimulation can be applied. Displayed results of the source signal can
147 be firing rates of the subpopulations, PSPs, LFP, or the mean mem-
148 brane potential of the layer V excitatory neurons using the EEG_view
149 module. Additionally, the time courses of parameter evolution and
150 stimulation signals are displayed in separate windows. The number of
151 NMMs and their parameters, parameter evolution, and the parameters
152 of the stimulation signal are saved in a user-named txt file, which can
153 be loaded for a new simulation.

154 • Whole-brain simulation: a Python script is available on the repository
155 to simulate 67 nodes starting from a previously saved simulation file
156 including parameter sets and evolutions, coupling matrices, and stimu-
157 lation. After loading the saved simulation files, the script can be modi-
158 fied to include parameter variations and stimulation signals on desired
159 nodes. Simulated network activity is projected to scalp electrodes. In
160 this projection the first node represented the thalamus was excluded,
161 since it is not considered in the lead field matrix.

162 After solving the system of differential equations, six different displays
163 appear: time courses and spectrogram of LFP signals, parameter evo-
164 lution, stimulation, and the time courses of EEG signal, as well as a
165 spatial projection of the source (LFP) signals onto the cortex 3D mesh.

166 As it is for the single node simulation, the whole-brain simulation can
167 be saved in a txt file, which can be loaded for a new simulation later
168 on.

169 • Network from scratch: a network of NMMs can be created and saved
170 for further simulations by defining the number of NMMs, the connec-
171 tivity and delay matrices, their parameter values and evaluations, and

172 stimulation signals. Similar to single node simulation, results of the nu-
173 merical integration, parameter evaluation, and stimulation signals can
174 be displayed. While eCOALIA uses by default the Colin head model,
175 the Desikan atlas, and lead field matrices for 66 cortical regions, the
176 user can replace them with other head models, brain atlases, and lead
177 field matrices.

178 *2.4. Software functionalities*

179 In this section we introduce briefly the functionalities of eCOALIA. Imple-
180 mentation details are given in the developer documentation (see Table 1).

181 *2.4.1. Parameter exploration*

182 The parameter evolution module enables the analysis of the model’s dynamics
183 in response to parameter variations. Users have the flexibility to define a
184 series of temporal points corresponding to specific parameter values in a
185 numpy list and choose the interpolation technique to infer parameter values
186 throughout the specified time span.

187 *2.4.2. Stimulation*

188 In order to mimic the impact of a certain type of brain stimulation (e.g.
189 transcranial electrical stimulation), eCOALIA includes a stimulation module.
190 The stimulation module enables applying an external stimulation to a single
191 NMM or concurrently to multiple ones. A stimulation signal perturbs the
192 membrane of the subpopulations of the NMMs if it is applied before the
193 sigmoid functions or the synapses if it is applied after the sigmoid functions.
194 The impact of the stimulation signal is scaled to differentiate the stimulation
195 impact on the subpopulation. The stimulation signal can take a diverse
196 range of forms (including sinusoidal, square, sawtooth, triangular, ramp,
197 chirp, or mono/biphasic pulses). Each form has different parameters, such as
198 amplitude, frequency, start time, and end time, that can be adjusted (Table
199 2) Furthermore, different types of stimulation signals can be combined if
200 applied on the same NMM to investigate potential synergistic effects.

201 *2.4.3. Selection of the scalp EEG*

202 The scalp EEG signal is computed by solving the forward problem, which cor-
203 responds to the projection of the source activity of size $N_R = 66$ onto the N_E
204 number of scalp EEG contacts (Section 2.2). Since the real EEG caps that are
205 available to clinicians and researchers have different numbers of contacts, the
206 eCOALIA user may want to develop pipelines including direct comparison be-
207 tween the simulation results and real recordings. For this, eCOALIA provides
208 8 different lead field matrices that correspond to artificial EEG caps contain-
209 ing different number of electrodes ($N_E = \{21, 32, 65, 110, 131, 200, 256, 257\}$).

Type of the stimulation	Required parameters
For all types	Starting time, end time
Constant	Amplitude
Sinus, Square, Sawtooth, Triangle	Amplitude, frequency, phase
Ramp	Starting amplitude, end amplitude
Sinus Ramp	Starting amplitude, end amplitude, frequency, phase
Square Pulse Biphasic	Amplitude, frequency, phase, pulse width
Chirp	Amplitude, starting frequency, end frequency, phase
Chirp Pulse	Amplitude, starting frequency, end frequency, phase, pulse width
Chirp Pulse Biphasic	Amplitude, starting frequency, end frequency, phase, pulse width
Square Pulse Rand	Amplitude, frequency, phase, pulse width
Square Pulse Biphasic Rand	Amplitude, frequency, phase, pulse width

Table 2: Stimulation forms and required parameters

210 *2.4.4. Displaying source signal on neocortex*

211 The Source View window projects the source activity on the cortex model and
212 displays the EEG contacts with their names around the cortex model. The
213 source activity is highlighted with a color code computed from the energy
214 in the frequency domain (delta, theta, alpha, beta, and gamma bands) or
215 amplitude domain (maximum, mean, and root mean square (RMS)). Time
216 evaluation of the source activity within a sliding window defined by the user
217 can be visualized by pressing the play button. This evaluation is performed
218 within a sliding window defined by the user, with the default being 1 second.
219 The Source View window contains sliding bars that allow the user to adjust
220 transparency and brightness. Additionally, the user can select from a variety
221 of color maps.

222 **3. Illustrative examples**

223 Usage of the software package is illustrated with two examples of whole-
224 brain simulation. The simulation files of these examples are available on
225 the GITHUB repository. The parameter sets are given in Supplementary
226 Material.

227 Figure 2 demonstrates a whole-brain simulation of a typical epileptic dis-
228 charge recorded during interictal periods (outside of seizures). In this exam-
229 ple, epileptic activity is associated with the right-precentral (r-PREC) region,

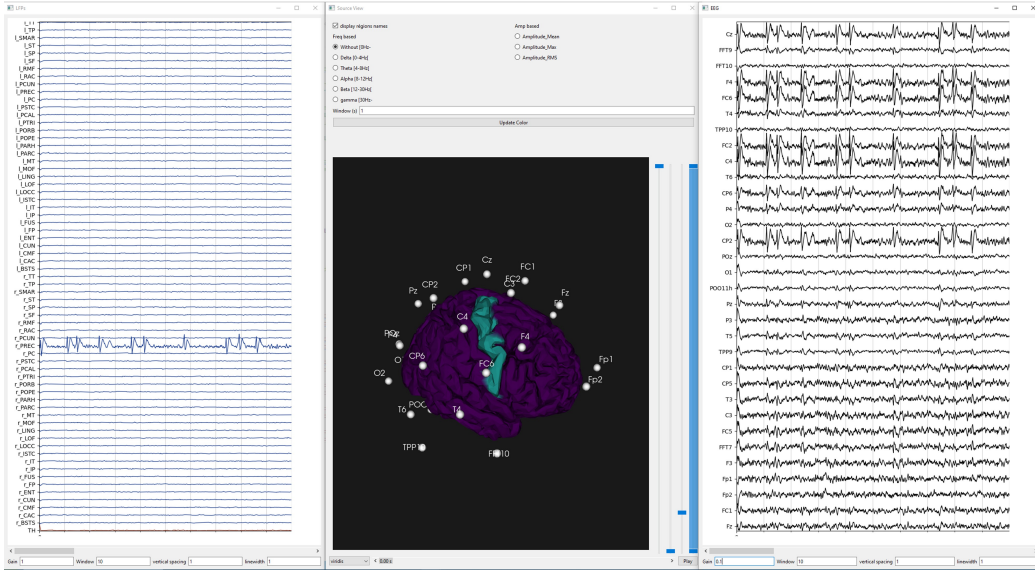


Figure 2: Whole-brain simulation of epileptic discharges. Left: Source activity given by local field potential. The right-precentral (r-PREC) region undergoes spike-and-wave discharges. Middle: Project of the source activity on the head model. The green region undergoes spike-and-wave discharges. Right: EEG signals measured by the scalp electrodes shown on the left panel. Corresponding simulation files is available on the code repository (Table 1) `src/SaveFiles/67NMM_spikewave_2.txt`.

230 as shown on LFP and Source View windows. The source signal is projected
 231 on 32 scalp-EEG channels as represented by markers positioned around the
 232 cortex. We can appreciate the large amplitude signals on the contacts closer
 233 to the r-PREC region, namely Cz, F4, FC6, FC2 C4, and CP2, as it can be
 234 verified.

235 The second example is a whole-brain simulation of a resting state and eyes-
 236 closed alpha band activity under healthy conditions (Fig 3). In this example,
 237 parameters of the left and right occipital lobes are changed in $t = [2, 7]$
 238 seconds to mimic the transition from resting state to eyes-closed alpha-band
 239 activity. The parameter evolution is visualized in the Parameter Evolution
 240 window. Notice that in this example we used an alpha-band filter and the
 241 coolwarm color code while demonstrating the alpha-band activity on the
 242 head model. The source signal is projected on 32-EEG channels.

243 4. Impact

244 Whole-brain modeling plays a key role in the discovery and analysis of elec-
 245 trophysiological signals [8, 9, 22, 10]. Despite this importance, modeling the

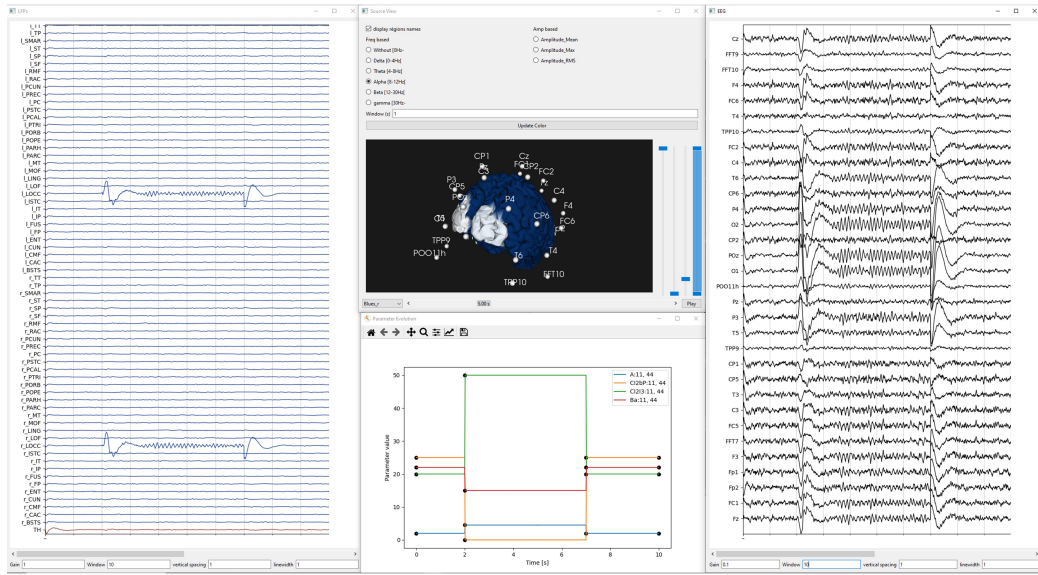


Figure 3: Whole-brain simulation of alpha-band oscillations. Left: Source activity given by local field potential. The left occipital lobe (l-LOCC) and the right occipital lobe (r-LOCC) undergo alpha-band oscillations in $t = [2, 7]$ seconds. Top middle: Project of the source activity on the head model with the occipital lobes in light blue. Bottom middle: The corresponding parameter evolution yielding these alpha-band activities. The legend indicates the indexes of the NMMs of which parameters were varied. In this example, the parameters A , $C_{I2b,P}$, $C_{I2,I3}$, and B_a of the 11th and 44th NMMs were modified. Right: EEG signals measured by the scalp electrodes shown on the left panel. Corresponding simulation files is available on the code repository (Table 1) `src/SaveFiles/67NMM_resting_alpha_4.txt`.

246 morphology of electrophysiological signals has been less of a concern of the
247 whole-brain modeling tools.

248 To address this challenge, we present eCOALIA, a Python-based modular
249 software. eCOALIA integrates a neurophysiologically plausible model of a
250 neocortical column that interacts via human connectome at the macroscale.
251 Parameter variation functionality allows the user to explore the parameter
252 space of eCOALIA. Stimulation signals can be used to test how electrical
253 stimulation can interact with cortical activity. 2-dimensional time and 3-
254 dimensional spatial representations of simulated activity simplify the inter-
255 pretation of simulations. Projection on EEG electrodes with different num-
256 bers of contacts can facilitate the comparison between the simulations and
257 available recorded signals. The modular structure of the software facilitates
258 further implementations and explorations.

259 Quantifying the similarity between simulated and real EEG signals is chal-
260 lenging due to asynchronous event timing, limiting the accuracy of classical
261 methods like cross-correlation. Although, the current version of the soft-
262 ware lacks direct tools for comparing real and simulated EEG signals, visual
263 inspection can still be useful. Additionally, the built-in spectrogram tool
264 allows frequency-based comparisons, helping assess whether both signals ex-
265 hibit similar rhythms and patterns. Further analytical methods, such as
266 coherence analysis or phase locking value, could improve this comparison
267 which would be implemented in future.

268 Different than the earlier version of the software [22], which simulates healthy
269 brain activity [14], eCOALIA can simulate both healthy and pathological
270 brain dynamics [12]. Therefore, it enables studying the impact of perturba-
271 tions caused by pathological activity on healthy ones, which is an asset for
272 brain research. By providing an *in silico* ground truth, eCOALIA can be
273 used to develop inverse solution methods for estimating cortical-level sources
274 [14, 24] or as a data-generator for training machine learning algorithms [25].

275 5. Conclusions

276 We introduced the eCOALIA software for neurophysiologically plausible mod-
277 eling of whole-brain dynamics. Thanks to the biophysical solution of the
278 forward problem, eCOALIA can simulate EEG signals by respecting the ob-
279 served morphology of pathophysiological events. eCOALIA advances the
280 realism of simulated EEG signals, interpretation of recordings, and patient-
281 specific whole-brain modeling.

282 **Acknowledgements**

283 This project has received funding from the European Research Council (ERC)
284 under the European Union’s Horizon 2020 research and innovation program
285 (Grant Agreement No. 855109).

286 **Declaration of competing interest**

287 Authors have no competing interest.

288 **References**

- 289 [1] K. Glomb, J. Cabral, A. Cattani, A. Mazzoni, A. Raj, B. Franceschiello,
290 Computational models in electroencephalography, *Brain Topogr* 35 (1)
291 (2022) 142–161. doi:10.1007/s10548-021-00828-2.
- 292 [2] G. Deco, A. Ponce-Alvarez, P. Hagmann, G. L. Romani, D. Mantini,
293 M. Corbetta, How local excitation–inhibition ratio impacts the whole
294 brain dynamics, *J Neurosci* 34 (23) (2014) 7886–7898, publisher: Society
295 for Neuroscience Section: Articles. doi:10.1523/JNEUROSCI.5068-13.
296 2014.
- 297 [3] G. Deco, V. Jirsa, A. R. McIntosh, O. Sporns, R. Kötter, Key role of
298 coupling, delay, and noise in resting brain fluctuations, *Proc Natl Acad*
299 *Sci* 106 (25) (2009) 10302–10307. doi:10.1073/pnas.0901831106.
- 300 [4] J. D. Griffiths, A. R. McIntosh, J. Lefebvre, A connectome-based, cor-
301 ticothalamic model of state- and stimulation-dependent modulation of
302 rhythmic neural activity and connectivity, *Front Comput Neurosci* 14
303 (2020). doi:10.3389/fncom.2020.575143.
- 304 [5] S. F. Muldoon, F. Pasqualetti, S. Gu, M. Cieslak, S. T. Grafton, J. M.
305 Vettel, D. S. Bassett, Stimulation-based control of dynamic brain net-
306 works, *PLOS Comput Biol* 12 (9) (2016) e1005076, publisher: Public
307 Library of Science. doi:10.1371/journal.pcbi.1005076.
- 308 [6] B. M. Jobst, R. Hindriks, H. Laufs, E. Tagliazucchi, G. Hahn, A. Ponce-
309 Alvarez, A. B. A. Stevner, M. L. Kringelbach, G. Deco, Increased sta-
310 bility and breakdown of brain effective connectivity during slow-wave
311 sleep: Mechanistic insights from whole-brain computational modelling,
312 *Sci Rep* 7 (1) (2017) 4634. doi:10.1038/s41598-017-04522-x.

- 313 [7] H. Endo, N. Hiroe, O. Yamashita, Evaluation of resting spatio-temporal
314 dynamics of a neural mass model using resting fMRI connectivity and
315 EEG microstates, *Front Comput Neurosci* 13 (2020). doi:10.3389/
316 fncom.2019.00091.
- 317 [8] P. Ritter, M. Schirner, A. R. McIntosh, V. K. Jirsa, The Virtual Brain
318 integrates computational modeling and multimodal neuroimaging, *Brain*
319 *Connectivity* 3 (2) (2013) 121–145. doi:10.1089/brain.2012.0120.
- 320 [9] P. Sanz Leon, S. Knock, M. Woodman, L. Domide, J. Mersmann,
321 A. McIntosh, V. Jirsa, The Virtual Brain: a simulator of primate brain
322 network dynamics, *Front Neuroinform* 7 (2013). doi:10.3389/fninf.
323 2013.00010.
- 324 [10] C. Cakan, N. Jajcay, K. Obermayer, *neurolib: a simulation framework*
325 *for whole-brain neural mass modeling*, *Cogn Comput* 15 (4) (2023) 1132–
326 1152. doi:10.1007/s12559-021-09931-9.
- 327 [11] E. Köksal-Ersöz, R. Lazazzera, M. Yochum, I. Merlet, J. Makhalova,
328 B. Mercadal, R. Sanchez-Todo, G. Ruffini, F. Bartolomei, P. Benquet,
329 F. Wendling, Signal processing and computational modeling for inter-
330 pretation of SEEG-recorded interictal epileptiform discharges in epilep-
331 togenic and non-epileptogenic zones, *J Neural Eng* 19 (5) (2022) 055005.
332 doi:10.1088/1741-2552/ac8fb4.
- 333 [12] F. Wendling, E. Koksall-Ersoz, M. Al-Harrach, M. Yochum, I. Merlet,
334 G. Ruffini, F. Bartolomei, P. Benquet, Multiscale neuro-inspired models
335 for interpretation of EEG signals in patients with epilepsy, *Clin Neuro-*
336 *physiol* 161 (2024) 198–210. doi:10.1016/j.clinph.2024.03.006.
- 337 [13] D. C. Van Essen, S. M. Smith, D. M. Barch, T. E. J. Behrens, E. Yacoub,
338 K. Ugurbil, The WU-Minn human connectome project: An overview,
339 *NeuroImage* 80 (2013) 62–79. doi:10.1016/j.neuroimage.2013.05.
340 041.
- 341 [14] J. Tabbal, A. Kabbara, M. Yochum, M. Khalil, M. Hassan, P. Benquet,
342 Assessing HD-EEG functional connectivity states using a human brain
343 computational model, *J Neural Eng* 19 (5) (2022) 056032. doi:10.
344 1088/1741-2552/ac954f.
- 345 [15] P. E. Kloeden, E. Platen, *Numerical solution of Stochastic Differ-*
346 *ential Equations*, Springer, Berlin, Heidelberg, 1992. doi:10.1007/
347 978-3-662-12616-5.

- 348 [16] P. L. Nunez, R. Srinivasan, *Electric fields of the Brain: The neurophysics*
349 *of EEG*, Oxford University Press, 2006. doi:10.1093/acprof:oso/
350 9780195050387.001.0001.
- 351 [17] S. Næss, G. Halnes, E. Hagen, D. J. Hagler, A. M. Dale, G. T. Einevoll,
352 T. V. Ness, Biophysically detailed forward modeling of the neural origin
353 of EEG and MEG signals, *NeuroImage* 225 (2021) 117467. doi:10.
354 1016/j.neuroimage.2020.117467.
- 355 [18] E. Lopez-Sola, R. Sanchez-Todo, E. Lleal, E. Köksal-Ersöz, M. Yochum,
356 J. Makhalova, B. Mercadal, M. Guasch-Morgades, R. Salvador,
357 D. Lozano-Soldevilla, J. Modolo, F. Bartolomei, F. Wendling, P. Ben-
358 quet, G. Ruffini, A personalizable autonomous neural mass model of
359 epileptic seizures, *J Neur Eng* 19 (5) (2022) 055002, publisher: IOP
360 Publishing. doi:10.1088/1741-2552/ac8ba8.
- 361 [19] C. J. Holmes, R. Hoge, L. Collins, R. Woods, A. W. Toga, A. C. Evans,
362 Enhancement of MR images using registration for signal averaging, *J*
363 *Comput Assist Tomo* 22 (2) (1998) 324.
- 364 [20] R. S. Desikan, F. Ségonne, B. Fischl, B. T. Quinn, B. C. Dicker-
365 son, D. Blacker, R. L. Buckner, A. M. Dale, R. P. Maguire, B. T.
366 Hyman, M. S. Albert, R. J. Killiany, An automated labeling sys-
367 tem for subdividing the human cerebral cortex on MRI scans into
368 gyral based regions of interest, *NeuroImage* 31 (3) (2006) 968–980.
369 doi:10.1016/j.neuroimage.2006.01.021.
- 370 [21] F. Tadel, S. Baillet, J. C. Mosher, D. Pantazis, R. M. Leahy, *Brainstorm:*
371 *a user-friendly application for MEG/EEG analysis*, *Comput Intel Neu-*
372 *rosc* 2011 (2011) e879716. doi:10.1155/2011/879716.
- 373 [22] S. Bensaid, J. Modolo, I. Merlet, F. Wendling, P. Benquet, COALIA: a
374 computational model of human EEG for consciousness research, *Front*
375 *Syst Neurosci* 13 (2019). doi:10.3389/fnsys.2019.00059.
- 376 [23] A. Gramfort, T. Papadopoulo, E. Olivi, M. Clerc, OpenMEEG: open-
377 source software for quasistatic bioelectromagnetics, *BioMed Eng OnLine*
378 9 (1) (2010) 45. doi:10.1186/1475-925X-9-45.
- 379 [24] E. Köksal-Ersöz, J. Makhalova, M. Yochum, C.-G. Bénar, M. Guye,
380 F. Bartolomei, F. Wendling, I. Merlet, Whole-brain simulation of in-
381 terictal epileptic discharges for patient-specific interpretation of in-
382 terictal SEEG data, *Neurophysiologie Clinique* 54 (5) (2024) 103005.
383 doi:10.1016/j.neucli.2024.103005.

384 [25] R. Sun, A. Sohrabpour, G. A. Worrell, B. He, Deep neural networks
385 constrained by neural mass models improve electrophysiological source
386 imaging of spatiotemporal brain dynamics, Proc Natl Acad Sci 119 (31)
387 (2022) e2201128119. doi:10.1073/pnas.2201128119.